Usami M., Mitsunaga K., Irie T., Miyajima A. Doi O.	Proteomic analysis of ethanol-induced embryotoxicity in cultured post-implantation rat embryos.	The Journal of Toxicological Sciences	39	285-292	2014
Usami M., Mitsunaga K., Miyajima A., Takamatu M., Kazama S., Irie T., Doi O., Takizawa T.	Effects of 13 developmentally toxic chemicals on the migration of rat cephalic neural crest cels in vitro.	Congenital Anomalies			2015
Irie T., Kikura-Hanajiri R., Usami M., Uchiyama N., Goda Y., Sekino Y	MAM-2201, a synthetic cannabinoid drug of abuse, suppresses the synaptic input to cerebellar Purkinje cells via activation of presynaptic CB1 receptors.	Neuropharmacology	95	479–91	2015
Oguchi-Katayama A., Monma A., Sekino Y., Moriguchi T., Sato K	Comparative gene expression analysis of the amygdalae of juvenile rats exposed to valproic acid at prenatal and postnatal stages.	J Toxicol Sci	38 (3)	381-402	2013
Takahashi K., Ishii-Nozawa R., Takeuchi K., Nakazawa K., Sekino Y., Sato K.	Niflumic acid activates additional currents of the human glial L-glutamate transporter EAAT1 in a substrate-dependent manner.	Biol Pharm Bull	36 (12)	1996-2004	2013
Fujimori, K., Takaki, J., Miura, M., Shigemoto-Mogami, Y., Sekino, Y., Suzuki, T., Sato, K.	Paroxetine prevented the down-regulation of astrocytic L-Glu transporters in neuroinflammation.	J Pharamcol Sci (in press)			
Shigemoto-Mogami, Y., Hoshikawa, K., Goldman, J.E.,Sekino, Y., Sato, K.	Microglia enhances neurogenesis and oligodendrogenesis in the early postnatal subventricular zone.	J Neurosci.	34(5)	2231-2243	2014
Shigemoto-Mogami, Y., Fujimori, K., Ikarashi, Y., Hirose, A., Sekino, Y., Sato, K.	Residual metals in carbon nanotubes suppress the proliferation of neural stem cells.	Fundam Toxcol Sci.	1(3)	87-94	2014
佐藤　薫	ミクログリアの発生と分化	Clinical Neuroscience	32 (12)	1338-1341	2015
Sato, K.	Microglia effects on neuronal development.	GLIA	63 (8)	1394-1495	2015
吉田祥子・穂積直裕	神経伝達物質を視るデバイスが拓く神経科学の展開 ～ 求められる技術を開発する技術 ～	信学技報	112-345	39-40	2012
吉田祥子・穂積直裕	発達期小脳アストロサイトの機能と秩序形成	JNNS.	20	14-18	2013

K. Watanabe, N. Takahashi, N. Hozumi, S. Yoshida,	Improvements in Enzyme-Linked Photo assay Systems for Spatiotemporal Observation of Neurotransmitter Release	Sensors and Materials	27 (10)	1035–1044	2015
H. Mabuchi, HY Ong, K. Watanabe, S. Yoshida, N. Hozumi,	Visualization of Spatially Distributed Bioactive Molecules Using Enzyme-Linked Photo Assay	IEEJ Transactions (in press)			
上野　晋	化学物質（金属・有機溶剤）の毒性学と産業医としての対応	産業医科大学雑誌	第35巻特集号	91-6	2013
Park EK, Wilson D, Choi HJ, Wilson CT, Ueno S.	Hazardous metal pollution in the republic of Fiji and the need to elicit human exposure.	Environ Health Toxicol.			2013
Obara G., Toyohira Y., Inagaki H., Takahashi K., Horishita T., Kawasaki T., Ueno S., Tsutsui M., Sata T., Yanagihara N.	Pentazocine inhibits norepinephrine transporter function by reducing its surface expression in bovine adrenal medullary cells.	*J Pharmacol Sci.*	121	138-47	2013
Uchida T., Furuno Y., Tanimoto A., Toyohira Y., Arakaki K., Kina-Tanada M., Kubota H., Sakanashi M., Matsuzaki T., Noguchi K. Nakasone J., Igarashi T., Ueno S., Matsushita M., Ishiuchi S., Masuzaki H., Ohya Y., Yanagihara N., Shimokawa H., Otsuji Y., Tamura M., Tsutsui M.	Development of an experimentally useful model of acute myocardial infarction: 2/3 nephrectomized triple nitric oxide synthases-deficient mouse.	J Mol Cell Cardiol.	77	29-41	2014
Horishita T., Yanagihara N., Ueno S., Sudo Y., Uezono Y., Okura D., Minami T., Kawasaki T., Sata T.	Neurosteroids allopregnanolone sulfate and pregnanolone sulfate have diverse effect on the a subunit of the neuronal voltage-gated sodium channels Nav1.2, Nav1.6, Nav1.7, and Nav1.8 expressed in *Xenopus* oocytes.	Anesthesiology.	121	620-631	2014
Okura D., Horishita T., Ueno S., Yanagihara N., Sudo Y., Uezono Y., Sata T.	The endocannabinoid anandamide inhibits voltage-gated sodium channels Nav1.2, Nav1.6, Nav1.7 and Nav1.8 in Xenopus oocytes.	Anesth. Analg.	118	554-62	2014
Yanagihara N, Zhang H, Toyohira Y, Takahashi K, Ueno S, Tsutsui M, Takahashi K.	New insights into the pharmacological potential of plant flavonoids in the catecholamine system.	J Pharmacol Sci.	124	123-8	2014

Inagaki H, Toyohira Y, Takahashi K, Ueno S, Obara G, Kawagoe T, Tsutsui M, Hachisuga T, Yanagihara N.	Effects of selective estrogen receptor modulators on plasma membrane estrogen receptors and catecholamine synthesis and secretion in cultured bovine adrenal medullary cells.	J Pharmacol Sci.	124	66-75	2014
Okura D., Horishita T., Ueno S., Yanagihara N., Sudo Y., Uezono Y., Minami T., Kawasaki T., Sata T.	Lidocaine preferentially inhibits the function of purinergic P2X7 receptors expressed in *Xenopus* Oocytes.	Anesth Analg.	120	597-605	2015
Ishidao T, Fueta Y, Ueno S, Yoshida Y, Hori H.	A cross-fostering analysis of bromine ion concentration in rats that that inhaled 1-bromopropane vapor.	*J. Occup. Health*, in press.			
Fueta Y, Kanemitsu M, Egawa S, Ishidao T, Ueno S, Hori H.	Prenatal exposure to 1-bromopropane suppresses kainate-induced wet dog shakes in immature rats.	*J UOEH.*	37	255-261	2015
Li X, Toyohira Y, Horisita T, Satoh N, Takahashi K, Zhang H, Iinuma M, Yoshinaga Y, Ueno S, Tsutsui M, Sata T, Yanagihara N.	Ikarisoside A inhibits acetylcholine-induced catecholamine secretion and synthesis by suppressing nicotinic acetylcholine receptor-ion channels in cultured bovine adrenal medullary cells.	*Naunyn Schmiedebergs Arch Pharmacol.*	388	1259-1269	2015

書籍

著者氏名	論文タイトル名	書籍全体の編集者名	書　籍　名	出版社名	出版地	出版年	ページ
Kanda Y.	Assessment of cigarette smoking toxicity using cancer stem cells.	Nazmi Sari	Smoking Restrictions, Risk Perceptions and Its Health and Environmental Impacts	Nova Science Publishers	United States of America	2014	185-196
Kanda Y.	1. Cancer Stem Cells - Fact or Fiction?	Dittmar T, Zänker KS	Role of Cancer Stem Cells in Cancer Biology and Therapy	CRC Press	United States of America	2013	1-22
諫田泰成	ヒトiPS細胞を用いた心毒性試験の現状と課題	安全性評価研究会編集委員会	谷本学校毒性質問箱第16号	株式会社サイエンティスト社	東京	2014	91-94
諫田泰成	再生心筋細胞を用いた安全性薬理評価系の開発	エイブル株式会社和田昌憲	再生医療における臨床研究と製品開発	技術情報協会	東京	2013	572-576

IV.　研究成果の刊行物・別刷

Metallomics

PAPER

View Article Online
View Journal

Cite this: DOI: 10.1039/c5mt00033e

Tributyltin induces mitochondrial fission through NAD-IDH dependent mitofusin degradation in human embryonic carcinoma cells

Shigeru Yamada,[a] Yaichiro Kotake,[b] Mizuho Nakano,[a] Yuko Sekino[a] and Yasunari Kanda*[a]

Received 4th February 2015,
Accepted 14th April 2015

DOI: 10.1039/c5mt00033e

www.rsc.org/metallomics

Organotin compounds, such as tributyltin (TBT), are well-known endocrine disruptors. TBT acts at the nanomolar level through genomic pathways *via* the peroxisome proliferator activated receptor (PPAR)/retinoid X receptor (RXR). We recently reported that TBT inhibits cell growth and the ATP content in the human embryonic carcinoma cell line NT2/D1 *via* a non-genomic pathway involving NAD^+-dependent isocitrate dehydrogenase (NAD-IDH), which metabolizes isocitrate to α-ketoglutarate. However, the molecular mechanisms by which NAD-IDH mediates TBT toxicity remain unclear. In the present study, we evaluated the effects of TBT on mitochondrial NAD-IDH and energy production. Staining with MitoTracker revealed that nanomolar TBT levels induced mitochondrial fragmentation. TBT also degraded the mitochondrial fusion proteins, mitofusins 1 and 2. Interestingly, apigenin, an inhibitor of NAD-IDH, mimicked the effects of TBT. Incubation with an α-ketoglutarate analogue partially recovered TBT-induced mitochondrial dysfunction, supporting the involvement of NAD-IDH. Our data suggest that nanomolar TBT levels impair mitochondrial quality control *via* NAD-IDH in NT2/D1 cells. Thus, mitochondrial function in embryonic cells could be used to assess cytotoxicity associated with metal exposure.

Introduction

Growing evidence suggests that environmental organometals contribute to the observed increase in neurodevelopmental disorders, such as learning disabilities, autism spectrum disorder, behavioral abnormalities and teratogenicity.[1–3] Since the developing brain is more vulnerable to injury than the adult brain, exposure to these organometals during early fetal development can cause permanent or delayed neural disorders at much lower doses than in adults.[4–7] Therefore, it is necessary to elucidate the cytotoxic effects of organometals at low levels during development.

Organotin compounds, such as TBT, are well known to cause various types of cytotoxicity *via* genomic and non-genomic pathways. In the genomic pathway, nanomolar concentrations of TBT activate the retinoid X receptor (RXR) and/or peroxisome proliferator-activated receptor γ (PPARγ) and result in neurodevelopmental defects in mammals.[8,9] Conversely, many reports have shown that TBT at micromolar levels causes mitochondorial toxicity in the non-genomic pathway. For example, micromolar TBT and dibutyltin (DBT) levels have been shown to prevent mitochondrial respiration by inhibiting the electron transfer from complexes I and III, and Mg-ATPase activity.[10–12] The non-genomic effect of TBT mediates cell death in rat neurons. TBT induces neuronal death *via* AMPK activation and the phosphorylation of the mammalian target of rapamycin (mTOR) in rat cortical neurons.[13,14] TBT also induces neuronal degeneration *via* mitochondria-mediated ROS generation in rat neurons.[15]

We studied nanomolar TBT toxicity using neuronal precursor NT2/D1 cells as a model of the neurodevelopmental stage[16] and found that nanomolar TBT levels inhibit intracellular energy metabolism, including ATP production, *via* mitochondrial NAD^+-dependent isocitrate dehydrogenase (NAD-IDH), which catalyzes the irreversible conversion of isocitrate to α-ketoglutarate in the tricarboxylic acid (TCA) cycle.[17,18] Based on these observations, we hypothesized that nanomolar TBT levels affect mitochondrial functions, thereby altering the energy metabolism of neuronal precursor cells.[19]

Mitochondria continuously change their morphology through fission and fusion. These mitochondrial dynamics are an important quality control mechanism that maintains mitochondrial function, such as ATP production.[20] Mitochondrial fission and fusion are regulated by several GTPases. In mitochondrial fusion, mitofusins 1 and 2 (Mfn1, 2) and optic atrophy 1 (Opa1) induce the fusion of the outer and inner mitochondrial membranes,

[a] *Division of Pharmacology, National Institute of Health Sciences, 1-18-1, Kamiyoga, Setagaya-ku 158-8501, Japan. E-mail: kanda@nihs.go.jp; Fax: +81-3-3700-9704; Tel: +81-3-3700-9704*

[b] *Department of Xenobiotic Metabolism and Molecular Toxicology, Graduate School of Biomedical and Health Sciences, Hiroshima University, Japan*

respectively.[21,22] The deletion of Mfn1 and Mfn2 in mice is embryonically lethal, and cells from these embryos contain fragmented and dysfunctional mitochondria.[23] In contrast, dynamin-related protein 1 (Drp1) is a cytoplasmic protein that assembles into rings surrounding the outer mitochondrial membrane, where it interacts with fission protein 1 (Fis1) to promote fission.[24,25]

In the present study, we have investigated the effect of TBT on mitochondrial quality control in NT2/D1 cells. We found that exposure to 100 nM TBT induced proteasomal degradation of Mfn and mitochondrial fragmentation through an NAD-IDH-dependent mechanism. Thus, impaired mitochondrial quality control is a novel mechanism of nanomolar level TBT-induced toxicity in human embryonic carcinoma cells.

Methods

Cell culture

NT2/D1 cells were obtained from the American Type Culture Collection (Manassas, VA, USA). The cells were cultured in Dulbecco's modified Eagle's medium (DMEM; Sigma-Aldrich, St Louis, MO, USA) supplemented with 10% fetal bovine serum (FBS; Biological Industries, Ashrat, Israel) and 0.05 mg ml^{-1} of the penicillin–streptomycin mixture (Life Technologies, Carlsbad, CA, USA) at 37 °C in 5% CO_2.

Assessment of mitochondrial fusion

After treatment with TBT (100 nM, 24 h), the cells were fixed with 4% paraformaldehyde and stained with 50 nM Mito-Tracker Red CMXRos (Cell Signaling Technology, Danvers, MA, USA) and 0.1 μg ml^{-1} 4′,6-diamidino-2-phenylindole (DAPI; Dojin, Kumamoto, Japan). Changes in the mitochondrial morphology were observed using confocal laser microscopy (Nicon A1). Images (n = 3–7) of random fields were obtained, and the number of cells displaying mitochondrial fusion (<10% punctiform) was counted in each image, as previously reported.[26]

Real-time PCR

Total RNA was isolated from NT2/D1 cells using the TRIzol reagent (Life Technologies), and quantitative real-time reverse transcription (RT)-PCR using a QuantiTect SYBR Green RT-PCR Kit (QIAGEN, Valencia, CA, USA) was performed using an ABI PRISM 7900HT sequence detection system (Applied Biosystems, Foster City, CA, USA), as previously reported.[27] The relative change in the amount of transcript was normalized to the mRNA levels of glyceraldehyde-3-phosphate dehydrogenase (GAPDH). The following primer sequences were used for real-time PCR analysis: human Drp1: forward, 5-TGGGCGCCGACATCA-3, reverse, 5-GCT CTGCGTTCCCACTACGA-3; human Fis1: forward, 5-TACGTCCG CGGGTTGCT-3, reverse, 5-CCAGTTCCTTGGCCTGGTT-3; human Mfn1: forward, 5-GGCATCTGTGGCCGAGTT-3, reverse, 5-ATTAT GCTAAGTCTCCGCTCCAA-3; human Mfn2: forward, 5-GCTCG GAGGCACATGAAAGT-3, reverse, 5-ATCACGGTGCTCTTCCCATT-3; human GAPDH: forward, 5-GTCTCCTCTGACTTCAACAGCG-3, reverse, 5-ACCACCCTGTTGCTGTAGCCAA-3.

Western blot analysis

Western blot analysis was performed as previously reported.[28] Briefly, the cells were lysed with cell lysis buffer (Cell Signaling Technology). The proteins were then separated by sodium dodecyl sulfate-polyacrylamide gel electrophoresis (SDS-PAGE) and electrophoretically transferred to Immobilon-P (Millipore, Billerica, MA, USA). The membranes were probed using the following antibodies: an anti-Mfn1 polyclonal antibody (1 : 1000; Cell Signaling Technology), an anti-Mfn2 monoclonal antibody (1 : 1000; Cell Signaling Technology), an anti-cytochrome c oxidase subunit IV (COX IV) monoclonal antibody (1 : 1000; Cell Signaling Technology), and an anti-β-actin monoclonal antibody (1 : 5000; Sigma-Aldrich). The membranes were then incubated with secondary antibodies against rabbit or mouse IgG conjugated to horseradish peroxidase (Cell Signaling Technology). The bands were visualized using the ECL western blotting analysis system (GE Healthcare, Buckinghamshire, UK), and images were acquired using a LAS-3000 imager (FUJIFILM UK Ltd., Systems, Bedford, UK).

Chemicals and reagents

Tributyltin chloride was obtained from Tokyo Chemical Industry (Tokyo, Japan). Tin acetate (TA), rosiglitazone (RGZ), CD3254,

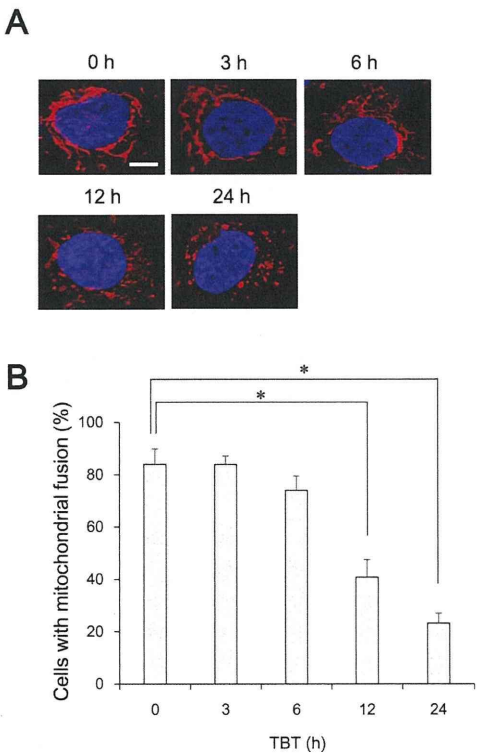

Fig. 1 Effect of TBT on the mitochondrial morphology in NT2/D1 cells. Cells were exposed to 100 nM TBT for 3, 6, 12, or 24 h. (A) The cells were stained with MitoTracker Red CMXRos and DAPI. Mitochondrial morphology was observed by confocal laser microscopy. Bar = 10 μm. (B) The number of cells undergoing mitochondrial fusion (<10% punctiform) was counted in each image. Data represent mean ± s.d. (n = 5). *P < 0.05.

apigenin, cycloheximide (CHX), carbonylcyanide m-chlorophenylhydrazone (CCCP), and MG132 were obtained from Sigma-Aldrich.

Statistical analysis

All data were presented as means ± S.D. ANOVA followed by a *post hoc* Tukey' test was used to analyze data in Fig. 1B, 2B, 3C, 4C, 5B, and 5C. Student's *t*-test was used to analyze data in Fig. 3A and 4B. *P*-values less than 0.05 were considered to be statistically significant.

Results and discussion

Effects of TBT on mitochondrial morphology

We have previously examined the effect of TBT (30–300 nM) on cell growth in NT2/D1 cells and found that TBT levels at the concentrations of 100 nM or more induced growth arrest in the cells.[17] Here we investigated whether 100 nM TBT affects mitochondrial dynamics in the cells. After exposure to 100 nM TBT for 12 h, we observed the increase in the number of cells with fragmented mitochondria, as compared to untreated control cells (Fig. 1A, B). After 24 h, the proportion of cells with mitochondrial fusion was nearly 80%. As a positive control, we used CCCP, which induces mitochondrial uncoupling and mitochondrial fission in other cells.[29] As expected, fragmented mitochondria were also observed following CCCP treatment for 24 h (Fig. 2A and B). In contrast, exposure to tin acetate (TA), which is less toxic, did not affect the mitochondrial morphology. To investigate whether TBT-induced mitochondrial fission was caused by changes in transcription, we treated the cells with the protein synthesis inhibitor cycloheximide. Treatment with cycloheximide did not alter the effects of TBT on the mitochondrial morphology (Fig. 2A and B). Moreover, rosiglitazone, an agonist of the TBT genomic target PPARγ, did not induce mitochondrial fragmentation. These results suggest that TBT induces mitochondrial fission through a non-genomic pathway in NT2/D1 cells.

TBT exposure induces proteasomal degradation of Mfn1 and 2

To examine the molecular mechanism by which TBT induces mitochondrial fragmentation, we assessed the effect of TBT on

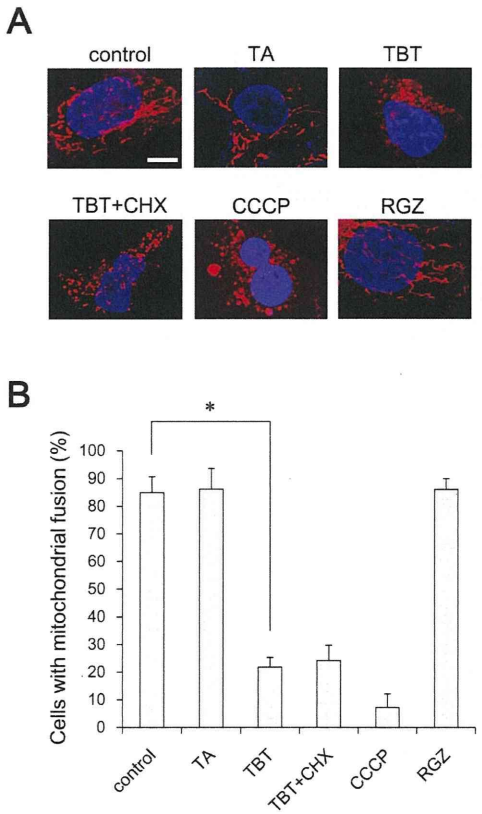

Fig. 2 Non-genomic effect of TBT-induced mitochondrial fission. Cells were exposed to 100 nM TA, 100 nM TBT, 100 nM TBT + 10 μg ml^{-1} cycloheximide (CHX), 1 μM CCCP or 100 nM rosiglitazone (RGZ) for 24 h. (A) The cells were stained with MitoTracker Red CMXRos and DAPI. Mitochondrial morphology was observed by confocal laser microscopy. Bar = 10 μm. (B) The number of cells undergoing mitochondrial fusion (<10% punctiform) was counted in each image. Data represent mean ± s.d. (n = 5). *P < 0.05.

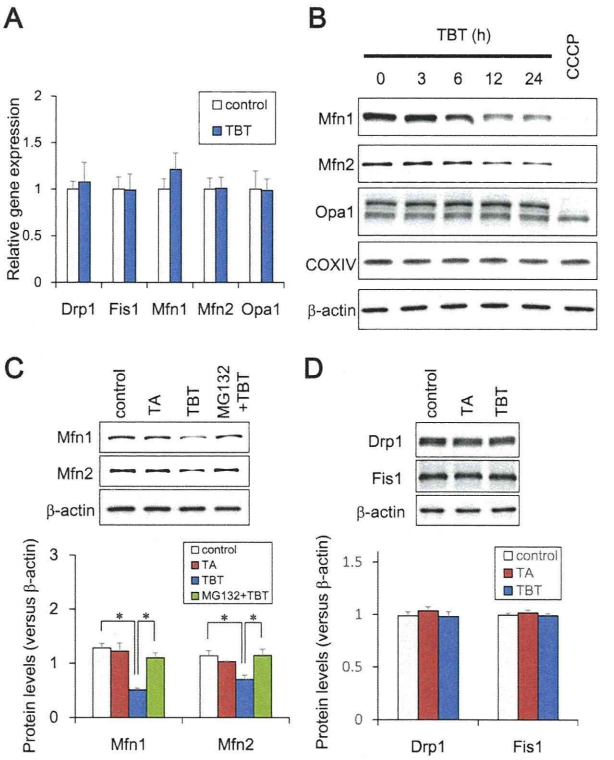

Fig. 3 Effect of TBT on mitochondrial protein levels in NT2/D1 cells. (A) After 24 h TBT exposure, the expression of mitochondrial genes was analyzed by real time PCR. The gene expression was not significantly altered by TBT exposure. (B) After TBT exposure for 3, 6, 12, or 24 h, mitochondrial proteins were analyzed by western blot using anti-Mfn1, Mfn2, Opa1, COXIV, or β-actin antibodies. (C) Cells were exposed to 100 nM TA, 100 nM TBT, or 100 nM TBT + 3 μM MG132 for 6 h. Mitochondrial proteins were analyzed by western blot using anti-Mfn1 or Mfn2 antibodies. (D) After 6 h TBT exposure, other mitochondrial proteins were analyzed by western blot using anti-Drp1, Fis1, or β-actin antibodies. Data represent mean ± s.d. (n = 3). *P < 0.05.

mitochondrial fission (Fis1, Drp1) and fusion genes (Mfn1, Mfn2, OPA1). Real-time PCR analysis showed that each gene expression was not significantly altered by TBT exposure (Fig. 3A). Fusion allows damaged mitochondria to incorporate into intact mitochondria, thereby maintaining mitochondrial function.[30] Dysfunctional mitochondria may lose their fusion capacity by the degradation of fusion proteins, resulting in the accumulation of fragmented mitochondria. Thus, we assessed the protein expression of Mfn1, Mfn2, and OPA1 in the presence or absence of TBT. Western blot analysis revealed that Mfn1 and Mfn2 protein levels were significantly reduced after 6 h, whereas OPA1 protein expression was not changed after 24 h (Fig. 3B and C). The other mitochondrial inner membrane protein, cytochrome *c* oxidase subunit IV (COX IV), was also not changed after 24 h (Fig. 3B). Moreover, MG132, a proteasome inhibitor, recovered the TBT-induced reduction in Mfn1 and Mfn2 (Fig. 3C). In contrast, the fusion proteins Fis1 and Drp1 were not affected by TBT (Fig. 3D). These data suggest that TBT-induced mitochondrial fragmentation is caused by the proteasomal degradation of Mfn1 and Mfn2.

Consistent with our data, chemical stressors have been reported to cause mitochondrial fission through the proteasomal degradation of Mfn. For example, doxorubicin induces ubiquitin-mediated proteasomal degradation of Mfn2, which facilitates mitochondrial fragmentation and apoptosis in sarcoma U2OS cells.[31] Another study has shown that CGP37157, an inhibitor of mitochondrial calcium efflux, mediates mitochondrial fission through Mfn1 degradation *via* ubiquitin ligase in prostate cancer LNCaP cells.[32] Since it remains unknown if ubiquitin ligases are involved or not in these TBT actions, further studies should be addressed to clarify the TBT-induced mechanism of proteasomal degradation of Mfn1 and Mfn2.

TBT induces mitochondrial defects *via* NAD-IDH

To investigate whether Mfn degradation and mitochondrial dysfunction are mediated through the non-genomic TBT target NAD-IDH, we examined the effects of apigenin, an NAD-IDH inhibitor,[33] on mitochondrial function. Apigenin (10 μM) decreased the number of cells undergoing mitochondrial fusion and induced mitochondrial fragmentation after 24 h (Fig. 4A and B). Furthermore, apigenin significantly reduced Mfn1 and Mfn2 protein expression, which was recovered by MG132 treatment (Fig. 4C). Apigenin has been reported to inhibit not only NAD-IDH but also hnRNPA2 and NF-κB.[33]

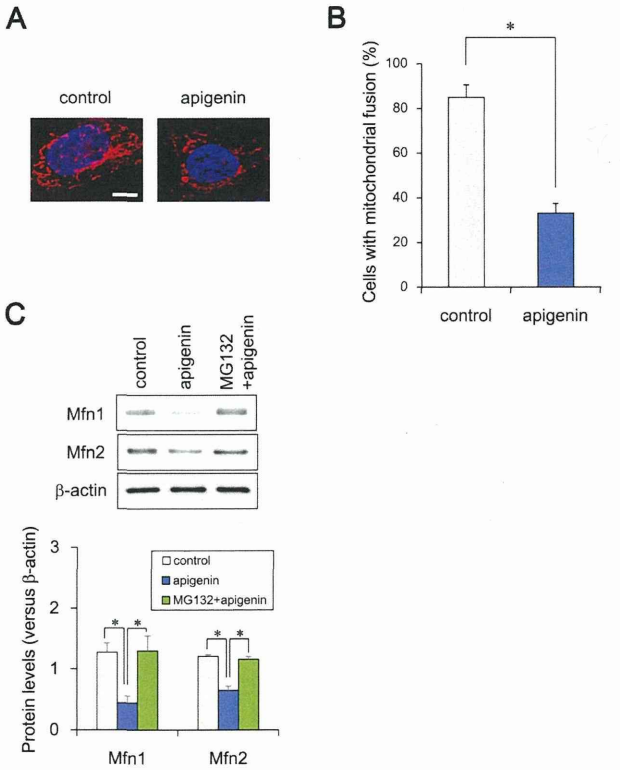

Fig. 4 Effect of apigenin on mitochondrial function in NT2/D1 cells. Cells were exposed to 10 μM apigenin. (A) Cells were stained with MitoTracker Red CMXRos and DAPI. Mitochondrial morphology was observed by confocal laser microscopy. Bar = 10 μm. (B) The number of cells undergoing mitochondrial fusion (<10% punctiform) was counted in each image. Data represent mean ± s.d. (n = 5). (C) Mitochondrial proteins in the cell lysate were analyzed by western blotting using anti-Mfn1 or Mfn2 antibodies. Data represent mean ± s.d. (n = 3). *P < 0.05.

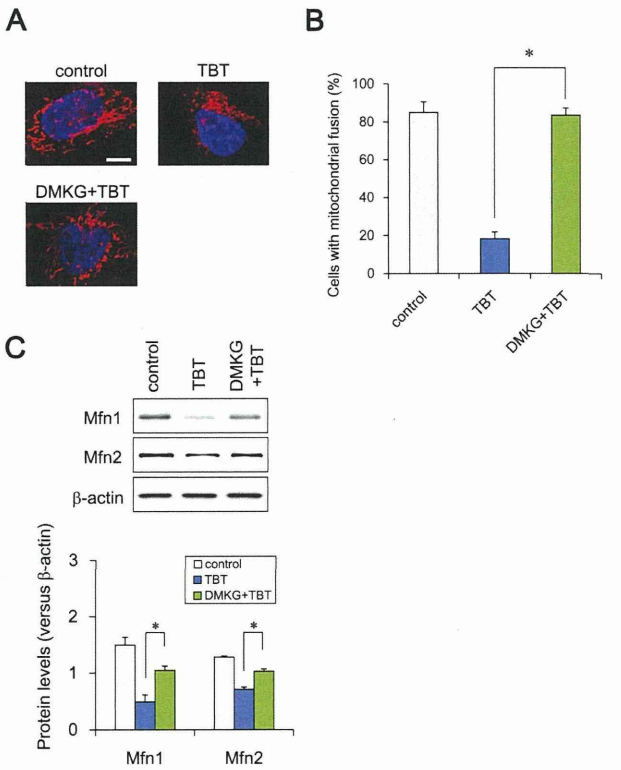

Fig. 5 Effect of DMKG on TBT-induced mitochondrial dysfunctions in NT2/D1 cells. Cells were exposed to 100 nM TBT and 7 mM DMKG. (A) Cells were stained with MitoTracker Red CMXRos and DAPI. Mitochondrial morphology was observed by confocal laser microscopy. Bar = 10 μm. (B) The number of cells undergoing mitochondrial fusion (<10% punctiform) was counted in each image. Data represent mean ± s.d. (n = 5). (C) Mitochondrial proteins were analyzed by western blotting using anti-Mfn1 or Mfn2 antibodies. Data represent mean ± s.d. (n = 3). *P < 0.05.

We cannot rule out the possibility that apigenin-induced mitochondrial dysfunction was induced by other targets. It is necessary to confirm our data by shRNA against NAD-IDH. To further confirm the involvement of NAD-IDH, we used dimethyl α-ketoglutarate (DMKG), a cell-permeable analog of α-ketoglutarate.[34] Incubation with DMKG prevented TBT-induced mitochondrial fragmentation in NT2/D1 cells (Fig. 5A) and recovered the number of cells undergoing mitochondrial fusion to the basal level (Fig. 5B). Furthermore, DMKG significantly recovered the TBT-induced the proteasomal degradation of Mfn1 and Mfn2 (Fig. 5C). Taken together, these data suggest that NAD-IDH mediates TBT-induced mitochondrial dysfunction *via* Mfn degradation in NT2/D1 cells. In addition to NAD-IDH, citrate synthase and α-ketoglutarate dehydrogenase also work as rate-limiting enzymes in the TCA cycle. Aluminium has been shown to induce oxidative stress *via* the negative regulation of citrate synthase and α-ketoglutarate dehydrogenase.[35,36] We could not rule out the possibility that TBT affects these enzymes. Several reports indicate that knockdown of Mfn1 and Mfn2 in the cells induces mitochondrial fragmentation and shows severe cellular defects, including decreased ATP content and poor cell growth.[30,37] Especially, Mfn2 has been reported to be necessary for striatal axonal projections of midbrain dopamine neurons by studies using dopamine neuron-specific Mfn2 knockout mice.[38] Taken together, Mfn1 and Mfn2 might be involved in several TBT actions *via* NAD-IDH, such as the reduction of ATP content, growth inhibition and enhancement of neuronal differentiation.

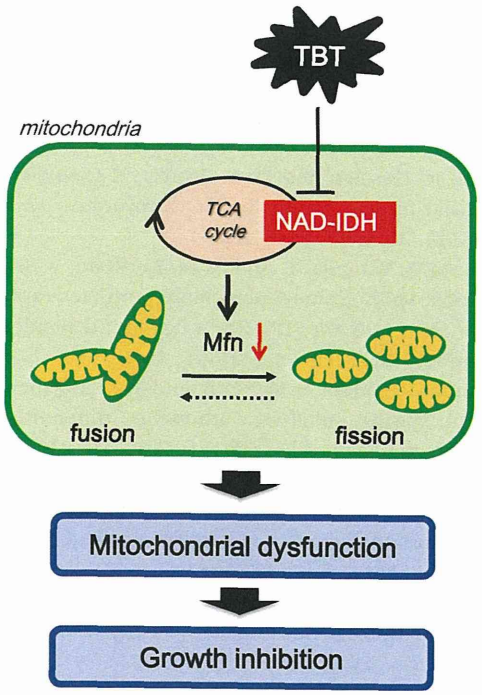

Fig. 6 Proposed model of TBT toxicity through non-genomic pathways in human embryonic carcinoma cells. Nanomolar TBT levels induce Mfn degradation and mitochondrial fission through NAD-IDH inhibition. These negative effects of TBT on mitochondrial quality control could mediate cell growth inhibition.

Conclusions

Based on our data, we have proposed a model of nanomolar TBT-induced mitochondrial dysfunction in neuronal precursor cells (Fig. 6). We demonstrated that TBT mediates the inhibition of NAD-IDH and the loss of mitochondrial quality control, representing a novel non-genomic pathway of TBT-induced toxicity. These negative effects of TBT on mitochondria could inhibit ATP production and cell growth. Since TBT at micromolar levels is known to cause neuronal degeneration *via* multiple mitochondrial defects, similar mitochondrial dysfunction might be also observed in immature neuronal precursor cells. We have previously revealed TBT-induced NAD-IDH inhibition in the rat brain. It would be interesting to study whether TBT-induced mitochondrial dysfunction *via* NAD-IDH might be also observed *in vivo*. We are now conducting experiments to determine how TBT degrades Mfn proteins both *in vitro* and *in vivo*. It remains to be determined if micromolar concentrations of TBT induce other mitochondrial dysfunctions in NT2/D1 cells and if the mechanisms pointed out here are selective for immature cells.

List of abbreviations

CCCP	Carbonylcyanide *m*-chlorophenylhydrazone
CHX	Cycloheximide
COX IV	Cytochrome *c* oxidase subunit IV
DAPI	4′,6-Diamidino-2-phenylindole
DMEM	Dulbecco's modified Eagle's medium
DMKG	Dimethyl α-ketoglutarate
Drp1	Dynamin-related protein 1
FBS	Fetal bovine serum
Fis1	Fission protein 1
GAPDH	Glyceraldehyde-3-phosphate dehydrogenase
Mfn	Mitofusin
NAD-IDH	NAD^+-dependent isocitrate dehydrogenase
Opa1	Optic atrophy 1
PPAR	Peroxisome proliferator activated receptor
RGZ	Rosiglitazone
RXR	Retinoid X receptor
TA	Tin acetate
TBT	Tributyltin
TCA	Tricarboxylic acid

Conflict of interest

The authors declare that there are no conflicts of interest.

Acknowledgements

This work was supported by a Health and Labour Sciences research grant from the Ministry of Health, Labour and Welfare, Japan (#H25-Kagaku-Ippan-002 to Y.Ka.), a grant-in-aid for scientific research from the Ministry of Education, Culture, Sports, Science, and Technology, Japan (#26293056, #26670041 to Y. Kanda), and a grant from the Smoking Research Foundation (Y. Kanda).

References

1 E. Dopp, L. M. Hartmann, A. M. Florea, A. W. Rettenmeier and A. V. Hirner, Environmental distribution, analysis, and toxicity of organometal(loid) compounds, *Crit. Rev. Toxicol.*, 2004, **34**, 301–333.

2 A. T. Gardlund, T. Archer, K. Danielsen, B. Danielsson, A. Frederiksson, N. G. Lindquist, H. Lindstrom and J. Luthman, Effects of prenatal exposure to tributyltin and trihexyltin on behavior in rats, *Neurotoxicol. Teratol.*, 1991, **13**, 99–105.

3 A. Mariani, R. Fanelli, A. Re Depaolini and M. De Paola, Decabrominated diphenyl ether and methylmercury impair fetal nervous system development in mice at documented human exposure levels, *Dev. Neurobiol.*, 2015, **75**, 23–38.

4 G. Winneke, Developmental aspects of environmental neurotoxicology: lessons from lead and polychlorinated biphenyls, *J. Neurol. Sci.*, 2011, **308**, 9–15.

5 L. G. Costa, M. Aschne, A. Vitalone, T. Syversen and O. P. Soldin, Developmental neuropathology of environmental agents, *Annu. Rev. Pharmacol. Toxicol.*, 2004, **44**, 87–110.

6 J. Dobbing, Vulnerable periods in developing brain, in *Appl. Neurochem*, ed. A. N. Davison and J. Dobbing, Davis, Philadelphia, 1968, pp. 287–316.

7 P. M. Rodier, Developing brain as a target of toxicity, *Environ. Health Perspect.*, 1995, **103**(suppl 6), 73–76.

8 T. Kanayama, N. Kobayashi, S. Mamiya, T. Nakanishi and J. Nishikawa, Organotin compounds promote adipocyte differentiation as agonists of the peroxisome proliferator-activated receptor gamma/retinoid X receptor pathway, *Mol. Pharmacol.*, 2005, **67**, 766–774.

9 M. Kajta and A. K. Wójtowicz, Impact of endocrine-disrupting chemicals on neural development and the onset of neurological disorders, *Pharmacol. Rep.*, 2013, **65**, 1632–1639.

10 H. S. Elsabbagh, S. Z. Moussa and O. S. El-tawil, Neurotoxicologic sequelae of tributyltin intoxication in rats, *Pharmacol. Res.*, 2002, **45**, 201–206.

11 S. Nesci, V. Ventrella, F. Trombetti, M. Pirini and A. Pagliarani, Tributyltin (TBT) and mitochondrial respiration in mussel digestive gland, *Toxicol. in Vitro*, 2011, **25**, 951–959.

12 S. Nesci, V. Ventrella, F. Trombetti, M. Pirini, A. R. Borgatti and A. Pagliarani, Tributyltin (TBT) and dibutyltin (DBT) differently inhibit the mitochondrial Mg-ATPase activity in mussel digestive gland, *Toxicol. in Vitro*, 2011, **25**, 117–124.

13 Y. Nakatsu, Y. Kotake, N. Takai and S. Ohta, Involvement of autophagy *via* mammalian target of rapamycin (mTOR) inhibition in tributyltin-induced neuronal cell death, *J. Toxicol. Sci.*, 2010, **35**, 245–251.

14 Y. Kotake, Molecular mechanisms of environmental organotin toxicity in mammals, *Biol. Pharm. Bull.*, 2012, **35**, 1876–1880.

15 S. Mitra, R. Gera, W. A. Siddiqui and S. Khandelwal, Tributyltin induces oxidative damage, inflammation and apoptosis *via* disturbance in blood–brain barrier and metal homeostasis in cerebral cortex of rat brain: an *in vivo* and *in vitro* study, *Toxicology*, 2013, **310**, 39–52.

16 M. Bani-Yaghoub, J. M. Felker and C. C. Naus, Human NT2/D1 cells differentiate into functional astrocytes, *NeuroReport*, 1999, **10**, 3843–3846.

17 S. Yamada, Y. Kotake, Y. Sekino and Y. Kanda, AMP-activated protein kinase-mediated glucose transport as a novel target of tributyltin in human embryonic carcinoma cells, *Metallomics*, 2013, **5**, 484–491.

18 S. Yamada, Y. Kotake, Y. Demizu, M. Kurihara, Y. Sekino and Y. Kanda, NAD-dependent isocitrate dehydrogenase as a novel target of tributyltin in human embryonic carcinoma cells, *Sci. Rep.*, 2014, **4**, 5952.

19 C. M. Nasrallah and T. L. Horvath, Mitochondrial dynamics in the central regulation of metabolism, *Nat. Rev. Endocrinol.*, 2014, **10**, 650–658.

20 R. J. Youle and A. M. van der Bliek, Mitochondrial fission, fusion, and stress, *Science*, 2012, **337**, 1062–1065.

21 T. Koshiba, S. A. Detmer, J. T. Kaiser, H. Chen, J. M. McCaffery and D. C. Chan, Structural basis of mitochondrial tethering by mitofusin complexes, *Science*, 2004, **305**, 858–862.

22 S. Cipolat, O. M. De Brito, B. Dal Zilio and L. Scorrano, OPA1 requires mitofusin 1 to promote mitochondrial fusion, *Proc. Natl. Acad. Sci. U. S. A.*, 2004, **101**, 15927–15932.

23 H. Chen, S. A. Detmer, A. J. Ewald, E. Erik, S. E. F. Griffin and D. C. Chan, Mitofusins mfn1 and mfn2 coordinately regulate mitochondrial fusion and are essential for embryonic development, *J. Cell Biol.*, 2003, **160**, 189–200.

24 E. Smirnova, L. Griparic, D.-L. Shurland and A. M. van der Bliek, Dynamin-related protein Drp1 is required for mitochondrial division in mammalian cells, *Mol. Biol. Cell*, 2001, **12**, 2245–2256.

25 Y. Yoon, E. W. Krueger, B. J. Oswald and M. A. McNiven, The mitochondrial protein hFis1 regulates mitochondrial fission in mammalian cells through an interaction with the dynamin-like protein DLP1, *Mol. Biol. Cell*, 2003, **23**, 5409–5420.

26 X. Fan, R. Hussien and G. A. Brooks, H_2O_2-induced mitochondrial fragmentation in C2C12 myocytes, *Free Radical Biol. Med.*, 2010, **49**, 1646–1654.

27 N. Hiarta, S. Yamada, T. Shoda, M. Kurihara, Y. Sekino and Y. Kanda, Sphingosine-1-phosphate promotes expansion of cancer stem cells *via* S1PR3 by a ligand-independent Notch activation, *Nat. Commun.*, 2014, **5**, 4806.

28 Y. Kanda, T. Hinara, S. W. Kang and Y. Watanabe, Reactive oxygen species mediate adipocyte differentiation in mesenchymal stem cells, *Life Sci.*, 2011, **89**, 250–258.

29 A. Tanaka, M. M. Cleland, S. Xu, D. P. Narendra, D. F. Suen, M. Karbowski and R. J. Youle, Proteasome and p97 mediate mitophagy and degradation of mitofusins induced by Parkin, *J. Cell Biol.*, 2010, **191**, 1367–1380.

30 H. Chen, A. Chomyn and D. C. Chan, Disruption of fusion results in mitochondrial heterogeneity and dysfunction, *J. Biol. Chem.*, 2005, **280**, 26185–26192.

31 G. P. Leboucher, Y. C. Tsai, M. Yang, K. C. Shaw, M. Zhou, T. D. Veenstra, M. H. Glickman and A. M. Weissman, Stress-induced phosphorylation and proteasomal degradation of mitofusin 2 facilitates mitochondrial fragmentation and apoptosis, *Mol. Cell*, 2012, **47**, 547–557.

32 V. Choudhary, I. Kaddour-Djebbar, R. Alaisami, M. V. Kumar and W. B. Bollag, Mitofusin 1 degradation is induced by a disruptor of mitochondrial calcium homeostasis, CGP37157: a role in apoptosis in prostate cancer cells, *Int. J. Oncol.*, 2014, **44**, 1767–1773.

33 D. Arango, K. Morohashi, A. Yilmaz, K. Kuramochi, A. Parihar, B. Brahimaj, E. Grotewold and A. I. Doseff, Molecular basis for the action of a dietary flavonoid revealed by the comprehensive identification of apigenin human targets, *Proc. Natl. Acad. Sci. U. S. A.*, 2013, **110**, E2153–E2162.

34 M. Willenborg, U. Panten and I. Rustenbeck, Triggering and amplification of insulin secretion by dimethyl alpha-ketoglutarate, a membrane permeable alpha-ketoglutarate analogue, *Eur. J. Pharmacol.*, 2009, **607**, 41–46.

35 D. R. Sharma, A. Sunkaria, W. Y. Wani, R. K. Sharma, R. J. Kandimalla, A. Bal and K. D. Gill, Aluminium induced oxidative stress results in decreased mitochondrial biogenesis *via* modulation of PGC-1α expression, *Toxicol. Appl. Pharmacol.*, 2013, **273**, 365–380.

36 R. J. Mailloux, J. Lemire and V. D. Appanna, Hepatic response to aluminum toxicity: dyslipidemia and liver diseases, *Exp. Cell Res.*, 2011, **317**, 2231–2238.

37 W. Yue, Z. Chen, H. Liu, C. Yan, M. Chen, D. Feng, C. Yan, H. Wu, L. Du, Y. Wang, J. Liu, X. Huang, L. Xia, L. Liu, X. Wang, H. Jin, J. Wang, Z. Song, X. Hao and Q. Chen, A small natural molecule promotes mitochondrial fusion through inhibition of the deubiquitinase USP30, *Cell Res.*, 2014, **24**, 482–496.

38 S. Lee, F. H. Sterky, A. Mourier, M. Terzioglu, S. Cullheim, L. Olson and N. G. Larsson, Mitofusin 2 is necessary for striatal axonal projections of midbrain dopamine neurons, *Hum. Mol. Genet.*, 2012, **21**, 4827–4835.

The Journal of Toxicological Sciences (J. Toxicol. Sci.)
Vol.41, No.2, 207-215, 2016

Original Article

Tributyltin induces G2/M cell cycle arrest via NAD$^+$-dependent isocitrate dehydrogenase in human embryonic carcinoma cells

Miki Asanagi[1,2,*], Shigeru Yamada[1,*], Naoya Hirata[1], Hiroshi Itagaki[2], Yaichiro Kotake[3], Yuko Sekino[1] and Yasunari Kanda[1]

[1]*Division of Pharmacology, National Institute of Health Sciences, 1-18-1 Kamiyoga, Setagaya-ku, Tokyo 158-8501, Japan*
[2]*Faculty of Engineering, Department of Materials Science and Engineering, Yokohama National University, 79-5 Tokiwadai, Hodogaya-ku, Yokohama, Kanagawa 240-8501, Japan*
[3]*Department of Xenobiotic Metabolism and Molecular Toxicology, Graduate School of Biomedical and Health Sciences, Hiroshima University, 1-2-3 Kasumi, Minami-ku, Hiroshima 734-8553, Japan*

(Received November 16, 2015; Accepted December 28, 2015)

ABSTRACT — Organotin compounds, such as tributyltin (TBT), are well-known endocrine-disrupting chemicals (EDCs). We have recently reported that TBT induces growth arrest in the human embryonic carcinoma cell line NT2/D1 at nanomolar levels by inhibiting NAD$^+$-dependent isocitrate dehydrogenase (NAD-IDH), which catalyzes the irreversible conversion of isocitrate to α-ketoglutarate. However, the molecular mechanisms by which NAD-IDH mediates TBT toxicity remain unclear. In the present study, we examined whether TBT at nanomolar levels affects cell cycle progression in NT2/D1 cells. Propidium iodide staining revealed that TBT reduced the ratio of cells in the G1 phase and increased the ratio of cells in the G2/M phase. TBT also reduced cell division cycle 25C (cdc25C) and cyclin B1, which are key regulators of G2/M progression. Furthermore, apigenin, an inhibitor of NAD-IDH, mimicked the effects of TBT. The G2/M arrest induced by TBT was abolished by NAD-IDHα knockdown. Treatment with a cell-permeable α-ketoglutarate analogue recovered the effect of TBT, suggesting the involvement of NAD-IDH. Taken together, our data suggest that TBT at nanomolar levels induced G2/M cell cycle arrest via NAD-IDH in NT2/D1 cells. Thus, cell cycle analysis in embryonic cells could be used to assess cytotoxicity associated with nanomolar level exposure of EDCs.

Key words: Embryonic carcinoma cells, Tributyltin, Cell cycle, Isocitrate dehydrogenase

INTRODUCTION

Organotin compounds, such as tributyltin (TBT) are typical environmental contaminants and are categorized as endocrine-disrupting chemicals (EDCs), which cause neurodevelopmental defects including behavioral abnormality and teratogenicity (Dopp *et al.*, 2004; Gårdlund *et al.*, 1991). Although the use of TBT has already been restricted, butyltin compounds, including TBT, can still be found in human blood at concentrations between 50 and 400 nM. There is still concern about TBT toxicity for human health (Whalen *et al.*, 1999).

Several studies have revealed that TBT activates retinoid X receptor (RXR) and/or peroxisome proliferator-activated receptor γ (PPARγ) (Kanayama *et al.*, 2005). TBT at nanomolar levels has the ability to bind with higher affinity than the intrinsic ligands and these genomic transcriptional activations have been reported to mediate neurodevelopmental defects in *Xenopus* (Yu *et al.*, 2011). In contrast, TBT elicits non-genomic pathway in mature rat neurons and brain tissues at nearly micromolar levels. For instance, TBT induces neuronal death by inhibiting mammalian target of rapamycin (mTOR) in rat cortical neurons (Nakatsu *et al.*, 2010). TBT also induces neuronal degeneration via the generation of reactive oxygen species along with marked reduction of GSH/GSSG levels in the rat brain (Mitra *et al.*, 2013).

Cell stress is known to trigger a checkpoint that arrests cells in the G1 or G2 phase (Gabrielli *et al.*, 2012). The cell cycle is tightly regulated by spatial and temporal

Correspondence: Yasunari Kanda (E-mail: kanda@nihs.go.jp)
*These authors equally contributed to this work.

expression of cell cycle proteins and divided into p53-dependent and p53-independent regulations (Shackelford *et al.*, 1999). In the p53-independent regulations, cdc25C phosphatase, a mitotic inducer, plays a central role in G2/M phase regulation. Cdc25C activates cyclin B1/cyclin-dependent kinase (Cdk) 1 complex, which triggers mitosis (Donzelli and Draetta, 2003) and cyclin B1 accumulates during the S and G2 phases, followed by nuclear translocation and association with Cdk1. Protein levels of these cell cycle regulators are strictly regulated during cell cycle progression. Ultraviolet irradiation or toxic drugs are known to cause G2 arrest by the inactivation of cyclin B1/Cdk1 via p53 induction followed by the upregulation of p21, a Cdk inhibitor and/or cdc25C downregulation by degradation (Chaudhary *et al.*, 2013; Kawabe, 2004; Nam *et al.*, 2010; Ouyang *et al.*, 2009).

We have previously reported that nanomolar levels of TBT induce growth arrest of neuronal precursor NT2/D1 cells as a model of neurodevelopmental stage (Yamada *et al.*, 2013). We found that TBT causes growth arrest via mitochondrial NAD^+-dependent isocitrate dehydrogenase (NAD-IDH), which catalyzes the irreversible conversion of isocitrate to α-ketoglutarate in the tricarboxylic acid (TCA) cycle (Yamada *et al.*, 2014). Based on these observations, we hypothesized that nanomolar levels of TBT could also affect cell cycle progression via NAD-IDH in NT2/D1 cells.

In the present study, we investigated the effect of TBT on cell cycle progression in NT2/D1 cells. We found that exposure to 100 nM TBT reduced the protein levels of cell cycle regulators and induced G2/M cell cycle arrest through an NAD-IDH-dependent mechanism. Thus, cell cycle regulation via NAD-IDH is a novel target of TBT-induced toxicity in human embryonic carcinoma cells.

MATERIALS AND METHODS

Cell culture

NT2/D1 cells were obtained from the American Type Culture Collection (Manassas, VA, USA). The cells were cultured in Dulbecco's modified Eagle's medium (DMEM; Sigma-Aldrich, St. Louis, MO, USA) supplemented with 10% fetal bovine serum (FBS; Biological Industries, Ashrat, Israel) and 0.05 mg/mL penicillin-streptomycin mixture (Life Technologies, Carlsbad, CA, USA) at 37°C in 5% CO_2.

Cell cycle analysis

The cells were trypsinized and harvested in phosphate buffered saline. Then the cells were resuspended in 70% ethanol for 30 min at -20°C. The fixed cells were collected by centrifugation and resuspended in propidium iodide (PI)/RNase Staining Buffer (BD Biosciences, San Jose, CA, USA) followed by incubation at room temperature for 30 min in the dark. Cell cycle distribution was determined by flow cytometric analysis of the DNA content using the BD FACS Aria II system (BD Biosciences). Data were analyzed by Modfit LT 4.0 (Verity Software House, Topsham, ME, USA).

Real-time PCR

Total RNA was extracted from NT2/D1 cells using TRIzol reagent (Life Technologies), and quantitative real-time reverse transcription (RT)-PCR was performed with QuantiTect SYBR Green RT-PCR Kit (QIAGEN, Valencia, CA, USA) using an ABI PRISM 7900HT sequence detection system (Applied Biosystems, Foster City, CA, USA) as previously reported (Hirata *et al.*, 2014). The relative change in transcript amounts was normalized to the expression levels of glyceraldehyde-3-phosphate dehydrogenase (GAPDH). The following primer sequences were used for real-time PCR analysis: human cdc25C: forward, 5′-AGGCAGCCTTGAGTTGCATAGAGA-3′, reverse, 5′-AGAGTTGGCTGGCTTGTGAGAAGA-3′;humancyclin B1:forward,5′-CGGGAAGTCACTGGAAACAT-3′,reverse, 5′-AAACATGGCAGTGACACCAA-3′; human GAPDH: forward, 5′-GTCTCCTCTGACTTCAACAGCG-3′, reverse, 5′-ACCACCCTGTTGCTGTAGCCAA-3′.

Western blot analysis

Western blot analysis was performed as previously reported (Kanda *et al.*, 2011). Briefly, cells were lysed with Cell Lysis Buffer (Cell Signaling Technology, Danvers, MA, USA). The proteins were then separated by sodium dodecyl sulfate-polyacrylamide gel electrophoresis (SDS-PAGE) and electrophoretically transferred to Immobilon-P membrane (Millipore, Billerica, MA, USA). The membranes were probed with an anti-cdc25C monoclonal antibody (1:1,000; Cell Signaling Technology), an anti-cyclin B1 monoclonal antibody (1:1,000; Cell Signaling Technology), and an anti-GAPDH polyclonal antibody (1:2,500; Abcam, Cambridge, UK) followed by incubation with horseradish peroxidase-conjugated secondary antibodies against rabbit or mouse IgG (Cel Signaling Technology). The bands were visualized using the ECL Western Blotting Analysis System (GE Healthcare, Buckinghamshire, UK), and images were acquired using a LAS-3000 Imager (FUJIFILM UK Ltd., Systems, Bedford, UK).

NAD-IDH activity assay

NAD-IDH activity was determined using the

Isocitrate Dehydrogenase Activity Colorimetric Assay Kit (Biovision, Mountain View, CA, USA), according to the manufacturer's instructions. Briefly, NT2/D1 cells were lysed in an assay buffer provided in the kit. The lysate was centrifuged at 14,000 *g* for 15 min, and the cleared supernatant was used for the assay.

NAD-IDHα knockdown

Knockdown studies were performed using NAD-IDHα shRNA lentiviruses from Sigma-Aldrich (MISSION shRNA) according to the manufacturer's protocol. A scrambled hairpin sequence was used as a negative control. Briefly, the cells were infected with the viruses at a multiplicity of infection of 10 in presence of 8 μg/mL hexadimethrine bromide (Sigma-Aldrich) for 24 hr, and were then subjected to selection with 0.5 μg/mL puromycin for 72 hr for further functional analyses.

Chemicals and reagents

Tributyltin Chloride was obtained from Tokyo Chemical Industry (Tokyo, Japan). Tin acetate (TA), apigenin, and dimethyl α-ketoglutarate (DMKG) were obtained from Sigma-Aldrich.

Statistical analysis

All data were presented as mean ± S.D. Analysis of variance (ANOVA) followed by post hoc Tukey's test was used to analyze the data in Figs. 1C, 1D, 1E, 2A, 2B, 3C, 4E, 5A, 5B, 6A and 6B. Student's t test was used to analyze the data in Figs. 3A, 3B, 4A, 4B and 4C. P-values less than 0.05 were considered to be statistically significant.

RESULTS

Effect of TBT on cell cycle progression

We have previously found that 100 nM TBT induced growth arrest in NT2/D1 cells (Yamada *et al.*, 2013). Here we investigated whether TBT affects cell cycle progression. Exposure to 100 nM TBT for 48 hr decreased the proportion of cells in the G1 phase (51.9% decrease) and increased of the proportion of cells in the G2/M phase (79.6% increase), compared with untreated control cells (Figs. 1A-E). In contrast, TBT did not affect the proportion of cells in the S phase. Moreover, exposure to tin acetate (TA), which is less toxic, did not affect cell cycle progression. These data suggest that TBT induces G2/M cell cycle arrest in the cells.

TBT exposure reduces G2/M cell cycle regulators, cdc25C and cyclin B1

To examine the molecular mechanism by which TBT induces G2/M cell cycle arrest, we assessed the protein levels of p53, a major cell cycle regulator. We found that p53 protein level was reduced after 24 hr of TBT treatment, whereas cisplatin, which is known to cause p53-dependent G2/M cell cycle arrest (Pani *et al.*, 2007), increased p53 levels (Supplementary Fig. 1). Since we could not observe p53-dependency in TBT-induced G2/M cell cycle arrest, we assessed cdc25C and its downstream factor, cyclin B1, which are also involved in G2/M progression of cell cycle. Western blot analysis revealed that cdc25C and cyclin B1 protein levels were reduced after 24 hr of TBT treatment (Fig. 2A). In contrast, exposure to TA did not affect cdc25C and cyclin B1 protein levels. Equal GAPDH protein expression levels were confirmed as a loading control. Next, we assessed the gene expression of cdc25C and cyclin B1. However, real-time PCR analysis showed that gene expression was not significantly altered by TBT exposure for both 24 and 48 hr (Fig. 2B). These data suggest that TBT-induced G2/M cell cycle arrest is caused by reduction of cdc25C and cyclin B1 proteins.

TBT induces G2/M cell cycle arrest via NAD-IDH

To investigate the molecular mechanisms by which cdc25C is degraded and G2/M cell cycle arrest is induced, we examined the effect of the PPARγ agonist rosiglitazone (RGZ), which is the genomic target of TBT. We found that RGZ did not induce G1 phase reduction and G2/M phase increase (Figs. 3A and B). RGZ at 100 nM induced PPARγ gene expression at similar level to 100 nM TBT in NT2/D1 cells (Fig. 3C), confirming the agonistic effect of RGZ on PPARγ expression described in previous report (Benkirane *et al.*, 2006). These data suggest that TBT induces G2/M cell cycle arrest in NT2/D1 cells through a non-genomic pathway. We next examined the involvement of the non-genomic target NAD-IDH. We used an NAD-IDH inhibitor apigenin (Arango *et al.*, 2013) at 10 μM, which reduced NAD-IDH activity to a level (22.4%) (Fig. 4A). As previously reported, 100 nM TBT had a similar inhibitory effect (24.4%; Yamada *et al.*, 2014). Treatment with apigenin (10 μM, 48 hr) decreased G1 phase ratio (58.6% decrease) and increased G2/M phase ratio (98.1% increase) (Figs. 4B and C). Similar to TBT, apigenin reduced protein expression of cdc25C and cyclin B1 without affecting gene expression (Figs. 4D and E). To further confirm the effect of apigenin, we performed knockdown (KD) experiments of NAD-IDHα, the catalytic subunit of NAD-IDH, using lentivirus-delivered shRNAs. Real-time PCR analysis showed that KD efficiency was approximately 40% (Yamada *et al.*, 2014). We could not obtain more highly KD cells because of cell

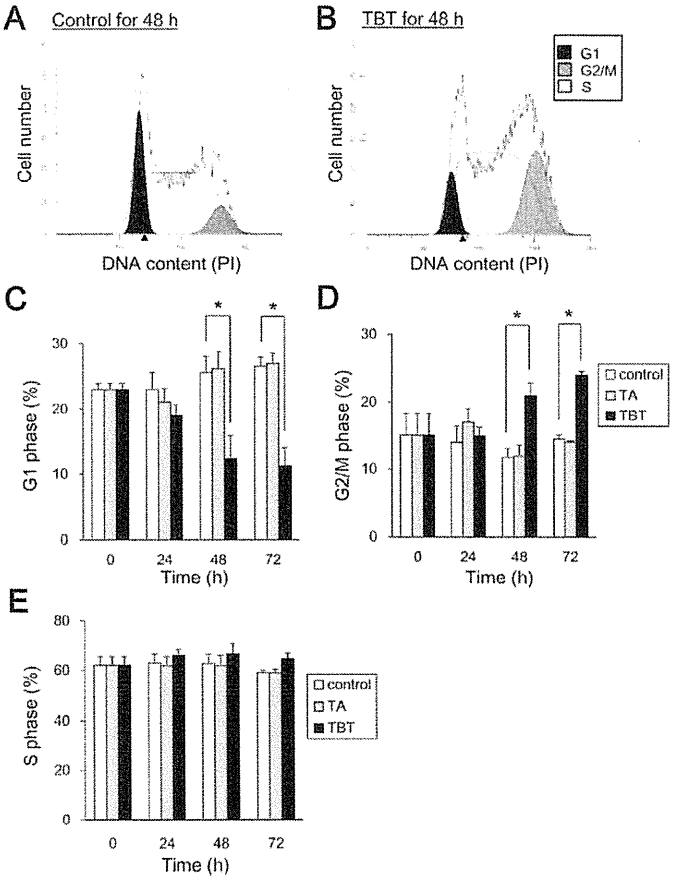

Fig. 1. Effect of TBT on cell cycle progression in NT2/D1 cells. Cells were exposed to 100 nM TA or TBT for 24, 48 or 72 hr. Cells were stained with propidium iodide (PI). Cell cycle distribution was determined by flow cytometric analysis of the DNA content on BD FACS Aria II. Representative cell cycle data in control (A) and TBT (B)-treated cells. The area ratio of G1 (C), G2/M (D) and S (E) phases was determined by Modfit LT 4.0. Data represent mean ± S.D. (n = 3). *P < 0.05.

death. Due to partial KD of the NAD-IDHα gene, NAD-IDH activity decreased by 22%, which is comparable to its decreased levels by TBT. In our previous studies, we observed that NAD-IDHα KD recovered the inhibitory effect of TBT on ATP content (Yamada *et al.*, 2014). This might be because the TBT target NAD-IDHα was already inhibited by shRNA and further inhibition by TBT was not observed in the knockdown cells. Similar to these data, NAD-IDHα KD abolished the TBT-induced G1 phase reduction and G2/M phase increase (Figs. 5A and B), suggesting the involvement of NAD-IDH on TBT effects. NAD-IDHα KD tended to decrease the proportion of cells in the G1 phase (24.1% ± 0.55 to 23.2% ± 0.34) and increase the proportion of cells in the G2/M phase (17.5% ± 1.6 to 20.3% ± 0.62), compared with control (Figs. 5A and B). Moreover, NAD-IDHα KD also abolished the TBT-induced reduction of cdc25C and cyclin B1 proteins (Fig. 5C). NAD-IDHα KD reduced the basal levels of cdc25C and cyclin B1 proteins, compared with control (Fig. 5C). These data suggest that NAD-IDH mediates TBT-induced G2/M cell cycle arrest in NT2/D1 cells. To further confirm the involvement of NAD-IDH, we treated the cells with dimethyl α-ketoglutarate (DMKG), a cell-permeable analog of α-ketoglutarate (Willenborg *et al.*, 2009). Incubation with DMKG prevented TBT-induced G2/M cell cycle arrest in NT2/D1 cells and

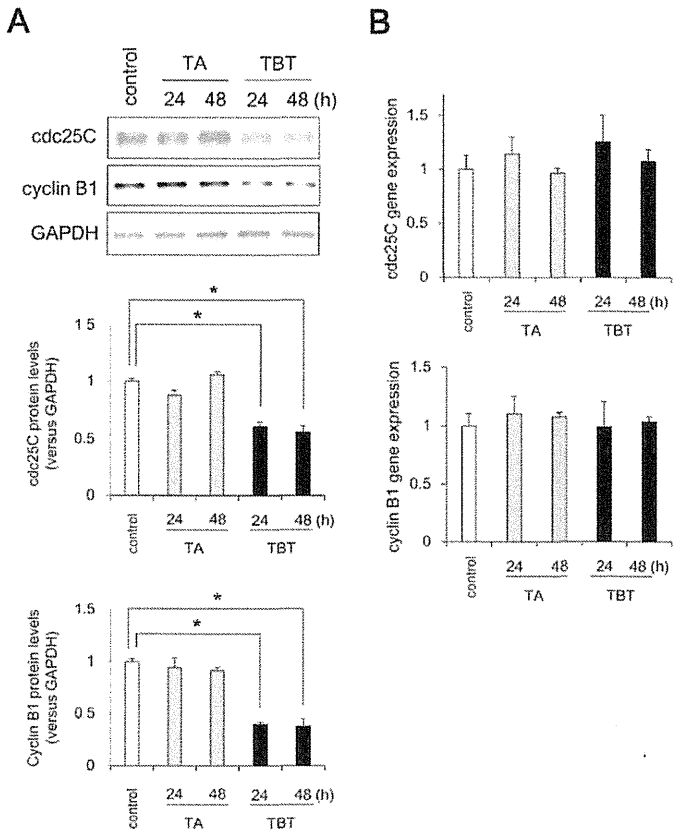

Fig. 2. Effect of TBT on expression levels of G2/M cell cycle regulators in NT2/D1 cells. After TBT exposure for 24 and 48 hr, protein expression was analyzed by western blot using anti-cdc25C, cyclin B1, or GAPDH antibodies (A). After TBT exposure for 24 or 48 hr, the expression of G2/M cell cycle regulators was analyzed by real time PCR (B). The gene expression was not significantly altered by TBT exposure. Data represent mean ± S.D. (n = 3).

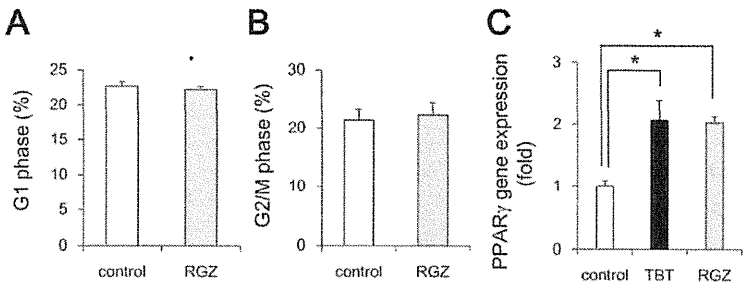

Fig. 3. Effect of RGZ on cell cycle progression in NT2/D1 cells. After RGZ exposure for 48 hr, cells were stained with propidium iodide (PI). The cell cycle distribution was determined by flow cytometric analysis of the DNA content using BD FACS Aria II. The ratio of G1 (A) and G2/M (B) phases was determined by Modfit LT 4.0. After exposure to TBT or RGZ, the expression of PPARγ was analyzed by real time PCR (C). The gene expression was comparably increased upon TBT or RGZ exposure. Data represent mean ± S.D. (n = 3). *P < 0.05.

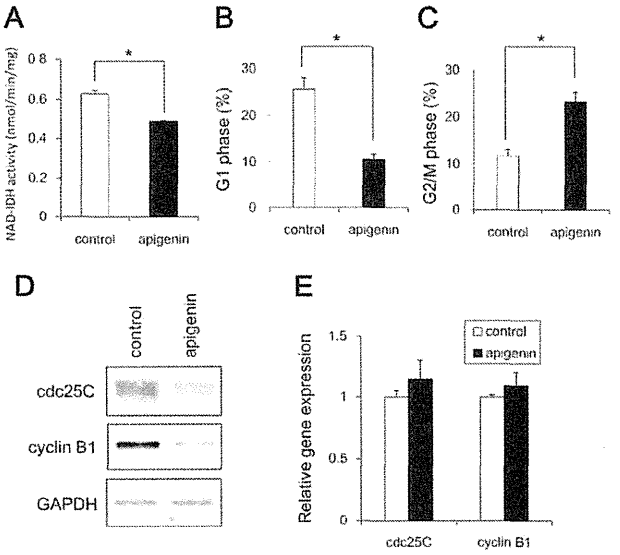

Fig. 4. Effect of apigenin on cell cycle progression in NT2/D1 cells. Cells were exposed to 10 μM apigenin for 24 hr and then determined NAD-IDH activity (A). Moreover, after exposure to apigenin for 48 hr, the cell cycle distribution was determined by flow cytometric analysis of the DNA content using BD FACS Aria II. The ratio of G1 (B) and G2/M (C) phases was determined by Modfit LT 4.0. The protein expressions in the cell lysate were analyzed by western blot using anti-cdc25C, cyclin B1, or GAPDH antibodies (D). The expression of G2/M cell cycle regulators was analyzed by real time PCR (E). The gene expression was not significantly altered upon apigenin exposure. Data represent mean ± S.D. (n = 3). *P < 0.05.

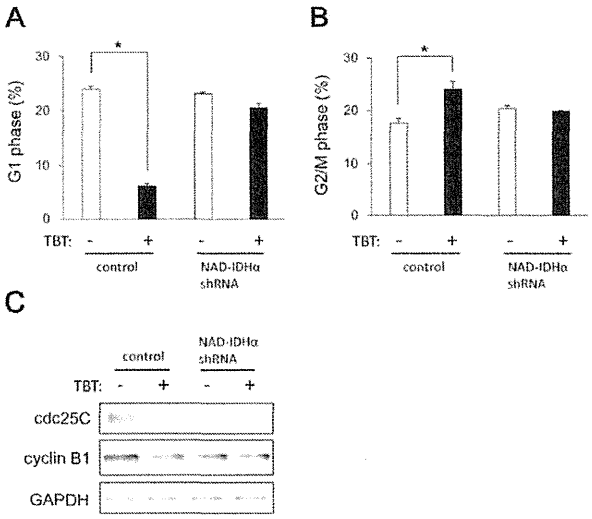

Fig. 5. Effect of NAD-IDH knockdown on cell cycle progression in NT2/D1 cells. Cells were infected with lentiviruses to express a shRNA against NAD-IDHα or a scrambled sequence shRNA (control). The infected cells were subjected to selection with 0.5 μg/mL puromycin for 72 hr and were then exposed to TBT at 100 nM for 48 hr. After staining with PI, cell cycle distribution was determined by flow cytometric analysis of the DNA content using BD FACS Aria II. The ratio of G1 (A) and G2/M (B) phases was analyzed by Modfit LT 4.0. The protein expressions in cell lysates were analyzed by western blot using anti-cdc25C, cyclin B1, or GAPDH antibodies (C). Data represent mean ± S.D. (n = 3). *P < 0.05.

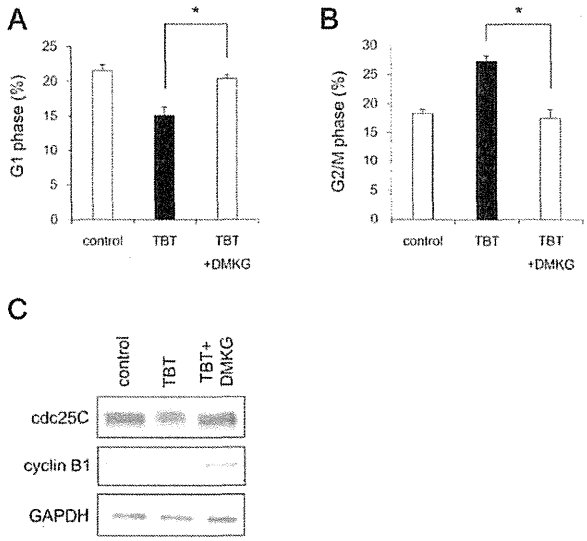

Fig. 6. Effect of dimethyl α-ketoglutarate (DMKG) on TBT-induced G2/M cell cycle arrest in NT2/D1 cells. Cells were exposed to 100 nM TBT and 7 mM DMKG for 48 hr. Cells were then stained with propidium iodide (PI) and cell cycle distribution was determined by flow cytometric analysis of the DNA content using BD FACS Aria II. The ratio of G1 (A) and G2/M (B) phases was analyzed by Modfit LT 4.0. Next, the protein expressions in cell lysates were analyzed by western blot using anti-cdc25C, cyclin B1, or GAPDH antibodies (C). Data represent mean ± S.D. (n = 3). *P < 0.05.

recovered the ratio of G1 and G2/M phases to the basal level (Figs. 6A and B). DMKG treatment also recovered TBT-induced protein reduction of cdc25C and cyclin B1 (Fig. 6C). Taken together, these data suggest that NAD-IDH mediates TBT-induced G2/M cell cycle arrest via cdc25C reduction in NT2/D1 cells.

DISCUSSION

Our data suggest that nanomolar TBT levels induce G2/M cell cycle arrest through the protein reduction of cdc25C and thereafter cyclin B1 (Figs. 1 and 2). Since the protein expression of p53 is decreased after TBT exposure, TBT-induced G2/M cell cycle arrest seems to be p53 independent. Consistent with our data, recent study has reported that nearly micromolar TBT levels induce G2/M cell cycle arrest in human amniotic cells via protein phosphatase (PP) 2A inhibition-mediated extracellular-signal-regulated kinase (ERK) inactivation (Zhang *et al.*, 2014). Since we did not observe the reduction of phospho-ERK in NT2/D1 cells after nanomolar levels of TBT exposure (data not shown), the mechanism of inducing G2 arrest may differ depending on the TBT levels and cell type. Moreover, several chemical stressors have been reported to cause G2/M cell cycle arrest through the protein reduction of cell cycle regulators (Chaudhary *et al.*, 2013; Nam *et al.*, 2010; Ouyang *et al.*, 2009). For instance, 4-Hydroxynonenal, an inducer of oxidative stress, causes DNA damage and induces G2/M cell cycle arrest in hepatocellular carcinoma HepG2 and Hep3B cells, following reduction of cdc25C and thereafter cyclin B1 proteins in a p53-independent manner (Chaudhary *et al.*, 2013). Reduction of cdc25C protein may be mediated by the ubiquitin-proteasome system in NT2/D1 cells. Cdc25C has been reported to be degraded via ubiquitination by BRCA1 during G2/M cell cycle arrest in breast cancer cell lines (Shabbeer *et al.*, 2013). During G2/M cell cycle arrest, another cell cycle regulators, such as Plk1, cdc25A and CDK1, are also known to be degraded by ubiquitin ligases, such as multi-subunit E3 ubiquitin ligases, Skp1-Cullin1-F-box Complex (SCF) or Anaphase Promoting Complex (APC) (Bassermann and Pagano, 2010). Further studies should determine whether ubiquitin ligases are involved in TBT-induced cdc25C reduction and subsequent G2/M cell cycle arrest in embryonic cells.

Our data using apigenin showed that TBT-induced G2/M cell cycle arrest is caused by NAD-IDH inhibition

(Fig. 4) and the data were verified by NAD-IDH knockdown and DMKG experiments (Figs. 5, 6). We used apigenin as a NAD-IDH inhibitor. We also confirmed the data by knockdown experiments. Since Apigenin has been reported to inhibit not only NAD-IDH but also hnRNPA2 and NF-κB (Arango *et al.*, 2013), we can not rule out the possibility that apigenin-induced G2/M cell cycle arrest was induced by other targets. Our previous report indicates that TBT induces mitochondrial dysfunction, such as impaired mitochondrial morphological dynamics and reduced ATP production via NAD-IDH in embryonic carcinoma cells (Yamada *et al.*, 2015). Considering that NAD-IDH is a mitochondrial enzyme, TBT-induced G2/M cell cycle arrest is caused by mitochondrial dysfunction through NAD-IDH inhibition. NAD-IDH catalyzes the reduction of NAD to NADH, which is oxidized by the electron transport chain and is required to generate proton electrochemical gradients across the inner mitochondrial membrane (Saraste, 1999). Thus, inhibition of NAD-IDH by TBT may reduce the NADH supply, thereby dissipating the proton electrochemical gradient. Intracellular Ca^{2+} may be also involved in mitochondrial dysfunction. Previous reports have shown that several anticancer drugs induce G2/M cell cycle arrest and apoptosis by depolarizing mitochondrial membrane potential and increasing intracellular Ca^{2+} (Fang *et al.*, 2014; Guo *et al.*, 2014). With respect to intracellular Ca^{2+}, there has been also reported that TBT induces mobilization of Ca^{2+} from intracellular stores and results in phosphorylation of MAPKs because its suppression by chelation of intracellular Ca^{2+} in human T lymphoblastoid cells (Yu *et al.*, 2000). Thus, Ca^{2+} release from depolarized mitochondria may induce G2/M cell cycle arrest after TBT exposure. Further studies should determine how the downstream signaling of NAD-IDH induces reduction of the cdc25C protein and subsequent G2/M cell cycle arrest after TBT exposure in embryonic cells.

In our previous studies, we have observed that TBT degrades mitofusin proteins and induces mitochondrial fission via the NAD-IDH inhibition. Moreover, we have also shown that TBT results in growth arrest by targeting the glycolytic systems (Yamada *et al.*, 2014). Both mitochondrial fission and glycolysis have been reported to be linked to cell cycle alterations (Yamamori *et al.*, 2015; Zhai *et al.*, 2013). Thus, we are currently investigating whether TBT-induced mitochondrial fission or glycolytic inhibition are linked to G2/M cell cycle arrest or not.

In summary, we demonstrate that TBT mediates G2/M cell cycle arrest through inhibition of NAD-IDH, representing a novel non-genomic pathway of TBT-induced toxicity (Fig. 7). These negative effects of TBT on the cell cycle could result in direct inhibition of cell growth. Thus, TBT-induced G2/M cell cycle arrest via NAD-IDH in embryonic cells may represent a novel mechanism of cytotoxicity associated with nanomolar level exposure of EDCs.

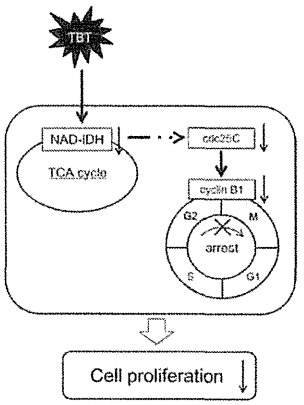

Fig. 7. Proposed model of TBT toxicity through non-genomic pathways in human embryonic carcinoma cells. Nanomolar TBT levels inhibit NAD-IDH activity. TBT induces G2/M cell cycle arrest via the protein reduction of cdc25C and its downstream target, cyclin B1. This TBT-induced G2/M cell cycle arrest may mediate cell growth inhibition.

ACKNOWLEDGMENTS

This work was supported by a Health and Labour Sciences Research Grant from the Ministry of Health, Labour and Welfare, Japan (#H25-Kagaku-Ippan-002 to Y. Kanda), a Grant-in-Aid for Scientific Research from the Ministry of Education, Culture, Sports, Science, and Technology, Japan (#26293056, #26670041 to Y. Kanda), the Research on Regulatory Harmonization and Evaluation of Pharmaceuticals, Medical Devices, Regenerative and Cellular Therapy Products, Gene Therapy Products, and Cosmetics from Japan Agency for Medical Research and development, AMED (To Y. Sekino), and a grant from the Smoking Research Foundation (Y. Kanda).

Conflict of interest---- The authors declare that there is no conflict of interest.

REFERENCES

Arango, D., Morohashi, K., Yilmaz, A., Kuramochi, K., Parihar, A., Brahimaj, B., Grotewold, E. and Doseff, A.I. (2013): Molecular basis for the action of a dietary flavonoid revealed by the com-

prehensive identification of apigenin human targets. Proc. Natl. Acad. Sci. USA, **110**, E2153-E2162.

Bassermann, F. and Pagano, M. (2010): Dissecting the role of ubiquitylation in the DNA damage response checkpoint in G2. Cell Death Differ., **17**, 78-85.

Benkirane, K., Amiri, F., Diep, Q.N., El Mabrouk, M. and Schiffrin, E.L. (2006): PPAR-gamma inhibits ANG II-induced cell growth via SHIP2 and 4E-BP1. Am. J. Physiol. Heart Circ. Physiol., **290**, H390-H397.

Chaudhary, P., Sharma, R., Sahu, M., Vishwanatha, J.K., Awasthi, S. and Awasthi, Y.C. (2013): 4-Hydroxynonenal induces G2/M phase cell cycle arrest by activation of the ataxia telangiectasia mutated and Rad3-related protein (ATR)/checkpoint kinase 1 (Chk1) signaling pathway. J. Biol. Chem., **288**, 20532-20546.

Donzelli, M. and Draetta, G.F. (2003): Regulating mammalian checkpoints through Cdc25 inactivation. EMBO Rep., **4**, 671-677.

Dopp, E., Hartmann, L.M., Florea, A.M., Rettenmeier, A.W. and Hirner, A.V. (2004): Environmental distribution, analysis, and toxicity of organometal(loid) compounds. Crit. Rev. Toxicol., **34**, 301-333.

Fang, C., Zhang, J., Qi, D., Fan, X., Luo, J., Liu, L. and Tan, Q. (2014): Evodiamine induces G2/M arrest and apoptosis via mitochondrial and endoplasmic reticulum pathways in H446 and H1688 human small-cell lung cancer cells. PLoS One, **9**, e115204.

Gabrielli, B., Brooks, K. and Pavey, S. (2012): Defective cell cycle checkpoints as targets for anti-cancer therapies. Front. Pharmacol., **3**, 9.

Gärdlund, A.T., Archer, T., Danielsen, K., Danielsson, B., Frederiksson, A., Lindquist, N.G., Lindström, H. and Luthman, J. (1991): Effects of prenatal exposure to tributyltin and trihexyltin on behaviour in rats. Neurotoxicol. Teratol., **13**, 99-105.

Guo, J., Zhao, W., Hao, W., Ren, G., Lu, J. and Chen, X. (2014): Cucurbitacin B induces DNA damage, G2/M phase arrest, and apoptosis mediated by reactive oxygen species (ROS) in leukemia K562 cells. Anticancer Agents Med. Chem., **14**, 1146-1153.

Hirata, N., Yamada, S., Shoda, T., Kurihara, M., Sekino, Y. and Kanda, Y. (2014): Sphingosine-1-phosphate promotes expansion of cancer stem cells via S1PR3 by a ligand-independent Notch activation. Nat. Commun., **5**, 4806.

Kanayama, T., Kobayashi, N., Mamiya, S., Nakanishi, T. and Nishikawa, J. (2005): Organotin compounds promote adipocyte differentiation as agonists of the peroxisome proliferator-activated receptor gamma/retinoid X receptor pathway. Mol. Pharmacol., **67**, 766-774.

Kanda, Y., Hinata, T., Kang, S.W. and Watanabe, Y. (2011): Reactive oxygen species mediate adipocyte differentiation in mesenchymal stem cells. Life Sci., **89**, 250-258.

Kawabe, T. (2004): G2 checkpoint abrogators as anticancer drugs. Mol. Cancer Ther., **3**, 513-519.

Mitra, S., Gera, R., Siddiqui, W.A. and Khandelwal, S. (2013): Tributyltin induces oxidative damage, inflammation and apoptosis via disturbance in blood–brain barrier and metal homeostasis in cerebral cortex of rat brain: an *in vivo* and *in vitro* study. Toxicology, **310**, 39-52.

Nakatsu, Y., Kotake, Y., Takai, N. and Ohta, S. (2010): Involvement of autophagy via mammalian target of rapamycin (mTOR) inhibition in tributyltin-induced neuronal cell death. J. Toxicol. Sci., **35**, 245-251.

Nam, C., Doi, K. and Nakayama, H. (2010): Etoposide induces G2/M arrest and apoptosis in neural progenitor cells via DNA damage and an ATM/p53-related pathway. Histol. Histopathol., **25**, 485-493.

Ouyang, G., Yao, L., Ruan, K., Song, G., Mao, Y. and Bao, S. (2009): Genistein induces G2/M cell cycle arrest and apoptosis of human ovarian cancer cells via activation of DNA damage checkpoint pathways. Cell Biol. Int., **33**, 1237-1244.

Pani, E., Stojic, L., El-Shemerly, M., Jiricny, J. and Ferrari, S. (2007): Mismatch repair status and the response of human cells to cisplatin. Cell Cycle, **6**, 1796-1802.

Saraste, M. (1999): Oxidative phosphorylation at the fin de siècle. Science, **283**, 1488-1493.

Shabbeer, S., Omer, D., Berneman, D., Weitzman, O., Alpaugh, A., Pietraszkiewicz, A., Metsuyanim, S., Shainskaya, A., Papa, M.Z. and Yarden, R.I. (2013): BRCA1 targets G2/M cell cycle proteins for ubiquitination and proteasomal degradation. Oncogene, **32**, 5005-5016.

Shackelford, R.E., Kaufmann, W.K. and Paules, R.S. (1999): Cell cycle control, checkpoint mechanisms, and genotoxic stress. Environ. Health Perspect., **107**, 5-24.

Whalen, M.M., Loganathan, B.G. and Kannan, K. (1999): Immunotoxicity of environmentally relevant concentrations of butyltins on human natural killer cells *in vitro*. Environ. Res., **81**, 108-116.

Willenborg, M., Panten, U. and Rustenbeck, I. (2009): Triggering and amplification of insulin secretion by dimethyl alpha-ketoglutarate, a membrane permeable alpha-ketoglutarate analogue. Eur. J. Pharmacol., **607**, 41-46.

Yamada, S., Kotake, Y., Sekino, Y. and Kanda, Y. (2013): AMP-activated protein kinase-mediated glucose transport as a novel target of tributyltin in human embryonic carcinoma cells. Metallomics, **5**, 484-491.

Yamada, S., Kotake, Y., Demizu, Y., Kurihara, M., Sekino, Y. and Kanda, Y. (2014): NAD-dependent isocitrate dehydrogenase as a novel target of tributyltin in human embryonic carcinoma cells. Sci. Rep., **4**, 5952.

Yamada, S., Kotake, Y., Nakano, M., Sekino, Y. and Kanda, Y. (2015): Tributyltin induces mitochondrial fission through NAD-IDH dependent mitofusin degradation in human embryonic carcinoma cells. Metallomics, **7**, 1240-1246.

Yamamori, T., Ike, S., Bo, T., Sasagawa, T., Sakai, Y., Suzuki, M., Yamamoto, K., Nagane, M., Yasui, H. and Inanami, O. (2015): Inhibition of the mitochondrial fission protein dynamin-related protein 1 (Drp1) impairs mitochondrial fission and mitotic catastrophe after X-irradiation. Mol. Biol. Cell, **26**, 4607-4617.

Yu, L., Zhang, X., Yuan, J., Cao, Q., Liu, J., Zhu, P. and Shi, H. (2011): Teratogenic effects of triphenyltin on embryos of amphibian (*Xenopus tropicalis*): a phenotypic comparison with the retinoid X and retinoic acid receptor ligands. J. Hazard Mater., **192**, 1860-1868.

Yu, Z.P., Matsuoka, M., Wispriyono, B., Iryo, Y. and Igisu, H. (2000): Activation of mitogen-activated protein kinases by tributyltin in CCRF-CEM cells: role of intracellular Ca(2+). Toxicol. Appl. Pharmacol., **168**, 200-207.

Zhai, X., Yang, Y., Wan, J., Zhu, R. and Wu, Y. (2013): Inhibition of LDH-A by oxamate induces G2/M arrest, apoptosis and increases radiosensitivity in nasopharyngeal carcinoma cells. Oncol. Rep., **30**, 2983-2991.

Zhang, Y., Go, Z. and Xu, L. (2014): Tributyltin induces a G2/M cell cycle arrest in human amniotic cells via PP2A inhibition-mediated inactivation of the ERK1/2 cascades. Environ. Toxicol. Pharmacol., **37**, 812-818.